JREE: Vol. 6, No. 1, (Winter 2019) 36-45

Journal of Renewable Energy and Environment

Journal Homepage: www.jree.ir

Research Article

Intelligent Pitch Angle Control Based on Gain-Scheduled Recurrent ANFIS

Ehsan Hosseini[a], Ehsan Aghadavoodi[a], Ghazanfar Shahgholian[b*], Homayoun Mahdavi-Nasab[b]

[a] *Smart Microgrid Research Center, Najafabad Branch, Islamic Azad University, Najafabad, Iran.*
[b] *Department of Electrical Engineering, Najafabad Branch, Islamic Azad University, Najafabad, Iran.*

PAPER INFO

Paper history:
Received 13 July 2019
Accepted in revised form 01 November 2019

Keywords:
Blade Pitch Angle Control
G-S RANFIS Controller
PI Controller
WECS

ABSTRACT

The effective utilization of wind energy conversion system (WECS) is one of the most crucial concerns for the development of renewable energy systems. In order to achieve appropriate wind power, different pitch angle methods are used. Recurrent Adaptive Neuro-Fuzzy Inference System (RANFIS) is utilized in this paper in a new effective design to improve the performance of classical and adaptive Proportional Integral (PI) controllers applied for the pitch control purposes. Adaptive-online performance and high robustness coverage are the main advantages of the suggested controller. The effectiveness of the proposed method is verified by a simplified two-mass wind turbine model and a detailed aero-elastic wind turbine simulator (FAST7). At any given wind speed, the proposed controller has outperformed PI, Adaptive Neuro-Fuzzy Inference System (ANFIS), and RANFIS based controllers, reducing the mechanical stress of drive train while presenting suitable aerodynamic power tracking and maintaining the rotational speed of the rotor under the rated value.

1. INTRODUCTION

Wind Energy Conversion Systems (WECS) play an important role in power production nowadays, and the number of wind farms has increased substantially in the last couple of decades [1,2]. Wind turbines are contributive sources of energy and can be exploited on MW scales [3,4]. To reach higher scales, the existence of efficient control systems is crucial [5,6]. Among wind turbine control systems employed to obtain the desired power from wind, the blade pitch angle control is the most dominant one [7,8]. This control is used to achieve the highest possible wind energy on the one side and the aerodynamic requirements for the generator on the other [9,10]. Dynamic performance of the system and fluctuations in the power system are directly connected to blade pitch angle control. Designing an adept pitch controller to track system changes at any given time is crucial. When the wind speed and, as a result, the turbine speed exceed their nominal values, the pitch controller activates and limits the wind power by increasing the angle [11,12]. For this purpose, numerous pitch control methods have been suggested, among which the PI controller is the most common one. PI controllers are simply designed regarding some linear models of the system at an operating point [13,14]. A PI controller with gain scheduling with respect to different operating points is the industry standard of pitch controls. Due to constant changes in wind speed, every controllable component is under uncertainties and disturbances [15,16]. Moreover, wind turbines are of the nonlinear systems, from which the operating point of the system changes in a broad range [17]. Therefore, the efficiency of the controllers designed based on a nominal point would reduce, which might weaken the dynamic response. For these reasons, PI controllers are not suitable for all operating points in the systems [18].

*Corresponding Author's Email: shahgholian@iaun.ac.ir (G. Shahgholian)

In recent years, various control methods including adaptive, robust, intelligent and variable structure control methods have been introduced for pitch control purpose [19,20]. Adaptive methods are the most important control methods adopted in recent decades. The purpose of applying such control methods is decreasing the sensitivity of the system in relation to changes in parameters. Adaptive controllers usually require a detailed model and a complex parameter estimator, which commonly leads to the limitation of these controllers [21]. The approach of robust controllers has been both improving dynamic response and functioning ineffectively in the case of changes in parameters. Although robust control methods are able to explain a good physical sense of the wind turbine, these methods need subsidiary controllers due to the non-linear modes of the wind turbine system [22]. According to the reasons mentioned, the efficiency of the classical and conventional controllers has made the intelligent methods more applicable [23,24]. The neural and fuzzy methods tuned by human experience or by evolutionary algorithms have become the most common control methods [25,26].

One of the first fuzzy controllers in wind turbines was introduced in the referenced study [27], which promoted both the system efficiency and economy by demonstrating its superiority in the dynamic response. In [28], the rotor speed variations and its derivatives are suggested besides the wind data as the controller inputs, where the need for anemometer is inevitable. A blade pitch controller for a two-MW wind turbine based permanent magnet generator was designed in the referenced study [29]. The replacement of the rotor speed as a controller input omits the need for wind data. Further, using the mechanical power besides the rotor speed as an input of the controller improves controller regarding uncertain modes. In [30], a Radial Basis Function (RBF) neural network was employed for adjusting the blade angle, where the power failure and its derivative forms were both considered as the inputs of the neural network. A control algorithm based on the ANFIS structure was proposed in [31] to set the power

coefficient of the wind turbine as a function of the tip-speed ratio and pitch angle. In [32], an ANFIS controller was applied to set the angle of input wind direction to the blades chord line. When the direction and intensity of the wind changes, the ANFIS utilizes a new learning procedure and adjusts control parameters to the new data, achieving more reliable performance in response to the rotor speed and the generator output power.

The proposed ANFIS pitch controller in [33] reduced the number of membership functions and unwanted rules in the fuzzy structure that decreased the neuro-fuzzy network complexity. Notwithstanding the strong wind tracking, it is an offline controller and needs to act adaptively.

In this paper, a G-S RANFIS controller is designed to specify PI parameters under a turbulent wind pattern. The presence of output signal control as an input of controller covers more nonlinear modes. The proposed controller works adaptively and online, where the PI gains are adjusted automatically and specified in accordance to the changes in the turbine parameters.

For a better clustering of the main controller, clustering is modified in the following three recurring stages:

1) Receiving the input-output of the PI controller data and building the initial FIS through the FCM algorithm and optimizing with the PSO algorithm;
2) Repeating the pattern of stages 1 with the ANFIS data;
3) Repeating the pattern of stages 2 with the recurrent ANFIS data to design the G-S RANFIS controller.

2. MODELING OF WIND TURBINES

In studying transient stability, for modeling the connection between the mechanical and electrical systems of wind turbines, the two-mass model is usually applied [34,35], which is expressed by the following relationships [36]:

$$\frac{d\omega_r}{dt} = \frac{1}{2H_R}(T_E + T_{sh}) \quad (1)$$

$$\frac{d\omega_t}{dt} = \frac{1}{2H_T}(T_M - T_{sh}) \quad (2)$$

$$\frac{d\theta}{dt} = \omega_b(\omega_t - \omega_r) \quad (3)$$

where the shaft twist angle is θ. T_E, T_S, T_M are the torques of the machine electromagnetic, the shaft torque, and mechanical turbine, respectively. The angular frequency of the turbine and rotor are ω_t and ω_r. The constant inertia of the rotor and turbine are H_R and H_T, respectively.

The mechanical torque of the turbine is stated as follows [37]:

$$T_M = \frac{0.5\,\rho\,\pi R^2 C_p V_W^3}{S_b\,\omega_T} \quad (4)$$

where S_b, ρ, V_w, and R are the base power, the air density, the wind speed, and the radius of the blade, respectively. The power coefficient (C_P) is commonly used to designate the efficiency of the entire turbine power system [38].

$$C_p = 0.22\ (\frac{116}{\lambda_i} - 0.4\beta_p - 5)\,e^{-\frac{12.5}{\lambda_i}} \quad (5)$$

λ_i is given by:

$$\lambda_i = (\frac{1}{\lambda + 0.08\beta_P} - \frac{0.035}{\beta_P^3 + 1})^{-1} \quad (6)$$

where β_P and λ are the pitch angle and the tip-speed ratio to wind speed, respectively:

$$\lambda = \frac{\omega_t R}{V_\omega} \quad (7)$$

As can be seen in (7), different wind speeds have their own rotational speeds [39]. By using the derivative of (5) and the extreme points of C_p, the optimum value of λ is obtained as follows [40]:

$$\lambda_{OPT} = (\frac{14.28 + 0.4\beta_P}{116} + \frac{0.035}{\beta_P^3})^{-1} - 0.8\beta_P \quad (8)$$

Under the nominal turbine wind speed, the rotational speed is selected in a way as to achieve C_{pmax}. In this mode, the control of the blades angle is inactive and the angles of the blades are set to zero. When the wind speed increases above the nominal value, the control of the blades angle is activated and the angle of the blades is set to limit the potential energy from the wind. Now, the desired power transforms to drive train and generator. Figure 1 shows the qualitative mechanical power curve versus varying wind speeds. Under the rated speed, the control approach is to obtain maximum power from the wind, because there is no pressure on the mechanical parts. In contrast, above the rated speed, the blades' angle controller is activated and increases the angle as the wind speed raises and, thus, limits the aerodynamic power.

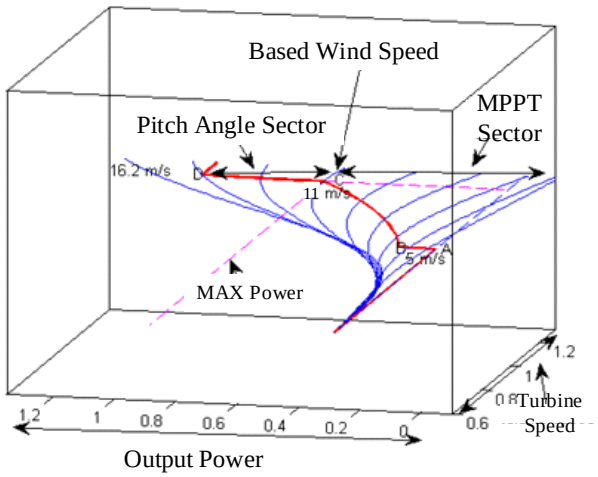

Figure 1. Power-speed characteristics of wind turbine.

Considering a time constant, τc, the delay between controller command and actuator movement can be presented by the system dynamic behavior as follows [41]:

$$\frac{d\beta}{dt} = \frac{1}{\tau_c}(-\beta_P + \beta_{ref}) \quad (9)$$

where β_{ref} is the reference pitch angle. Depending on τ_c ([0.2 to 0.25] up to turbine parameters) [42], the real controller output could be sought. When the wind speed is less than the nominal value, β_{pref} is kept at zero; when it exceeds the nominal value, the PI controller determines the real power as follows [43]:

$$\beta_{p\,ref} = K_{P\beta}(P - P_{ref}) + x_\beta \quad (10)$$

$$\frac{dx_\beta}{dt} = K_{I\beta}(P - P_{ref}) \quad (11)$$

where P is the mechanical power, and $K_{P\beta}$ and $K_{I\beta}$ are the proportional and integral control coefficients, respectively.

Figure 2 shows the block diagram of a common pitch angle control system, where the pitch servo is included. In this block diagram, X could be the rotor speed or the output power of the generator.

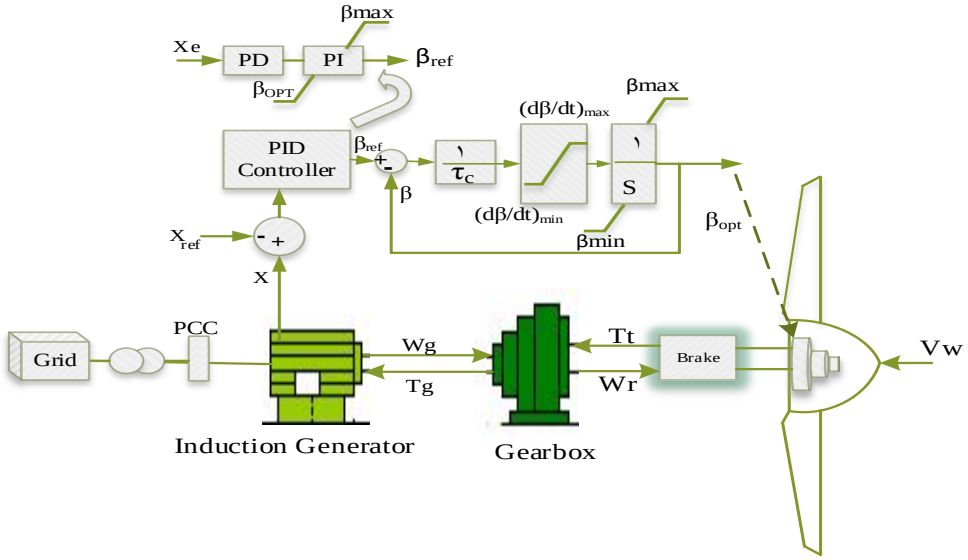

Figure 2. Block diagram of the PID, pitch angle control system.

3. ANFIS-BASED CONTROLLER DESIGN

3.1. Fuzzy C-means clustering method

Fuzzy C-means (FCM) is a data clustering method that omits the need for human experience in a fuzzy design, which therefore lowers the complexity of the neuro-fuzzy system and improves the efficiency. Based on an objective function (O.f), the FCM determines the cluster centers and membership functions. In an iterative algorithm, the appropriate values are attained to minimize the O.f. In the formulation of the clustering problem, the following components are used (supposing *k* clusters and *n d*-dimensional data) [44]:

Data: $x_1, x_2, \ldots, x_n \in R^d$

Cluster centers: $c_1, c_2, \ldots, c_k \in R^d$

Clusters: $A_1, A_2, \ldots, A_k$

$$x_i \in \mathbf{A}_j \Leftrightarrow j = \text{argmin } D(x_i, c_l) \quad (12)$$

where x_i is a member of cluster A_j if its distance to A_j cluster center is less than the distance to all other cluster centers. In fact, here, clusters compete to take possession of the data. The cluster centers and data distances must have a minimum value; therefore, the O.f could be written as:

$$O.f = \sum D[x_i, c_j(i)] = \frac{1}{n}\sum D[(x_i, c_j(i)]^2 \quad (13)$$

The degree of membership of x_i to the j^{th} cluster is expressed as follows:

$$u_j(x) = \frac{1}{\sum_k [\frac{D(c_j, x)}{D(c_k, x)}]^{\frac{2}{m-1}}} \quad 0 \le u_j(x) \le 1 \quad (14)$$

$$O.f = \frac{1}{n}\sum D(x_i, c_j(i))^2 * u_j(x) \quad (15)$$

Then, this is normalized as:

$$\begin{cases} u_j(x) = \dfrac{u_j(x)}{\sum_k u_k(x)} \\ \sum_j u_j(x) = 1 \end{cases} \quad (16)$$

All the centers, c_j, are expressed by the following equation:

$$c_j = \frac{[\sum_i u_j(x)]x_i}{\sum_i u_j(x)} \quad (17)$$

3.2. The inference system

To benefit the advantages of both neural networks and fuzzy systems, ANFIS has introduced a five-layer neuro-fuzzy inference system, represented by (18) to (23), as follows [45,46].

Layer 1: the i^{th} node yields a degree of membership for a linguistic variable, e.g., the function:

$$Q_i^1 = \mu_{Ai}(x) = \frac{1}{1+[(\frac{x-c_i}{\sigma_i})^2]^{b_i}} = \exp\frac{-0.5(x-c_j)^2}{\sigma_j^2} \quad (18)$$

where A_i is the linguistic variable, b_i , c_i, and σ_i form the membership function parameters, and *x* is the node input.

Layer 2: Considering the fuzzy rules as:

Rule i: if x_1 is A_i and x_2 is B_i, then $Y_i = a_i x_1 + b_i x_2 + c_i$

Each node output presents the firing power of its rule based on the relation [47]:

$$Q_i^2 = W_i = \mu_{Ai}(x).\mu_{Bi}(y) \quad (19)$$

Layer 3: Each node produces the relative firing power of the rule regarding the powers of all rules as follows:

$$Q_i^3 = \overline{W}_i = \frac{w_i}{\sum w_j} \quad (20)$$

Layer 4: Every node in this layer performs a function, defined as follows:

$$Q_i^4 = \overline{W}_i Y_i = \overline{W}_i .(a_i x_1 + b_i x_2 + c) \quad (21)$$

where $\overline{W_i}$ is the output of the third layer. In this article, the above linear method is applied in the SUGENO fuzzy structure.

Layer 5: the single node of this layer computes the final system output as a linear combination of all the previous layers' signals as follows [48]:

$$Q_i^5 = \text{OverallOutput} = \sum \overline{W}_i Y_i = \frac{\sum w_i Y_i}{\sum w_i} \quad (22)$$

If the neuro-fuzzy structure is assumed to be a two-input one-output system (as in Figure 3), for each x_t, the error is determined by P_{ref} and $P_{(t)}$, and the system cost function is defined as follows [49]:

$$E = \frac{1}{N}\sum_{t=1}^{T} e_t^2 \quad (23)$$

β_{ref} is calculated as:

$$\beta_{ref} = \frac{\sum_r [\sum_{j=1}^{m}(a_j x_1 + b_j x_2 + c_j) \exp(-\frac{1}{2}\sum_{i=1}^{n}\left(\frac{x_i - c_i}{\sigma}\right)^2)]}{\sum_r \exp(-\frac{1}{2}\sum_{i=1}^{n}\left(\frac{x_i - c_i}{\sigma}\right)^2)} \quad (24)$$

Finally, in order to acquire adaptive states for the tunable input-output, the PSO algorithm is used according to the following [50].

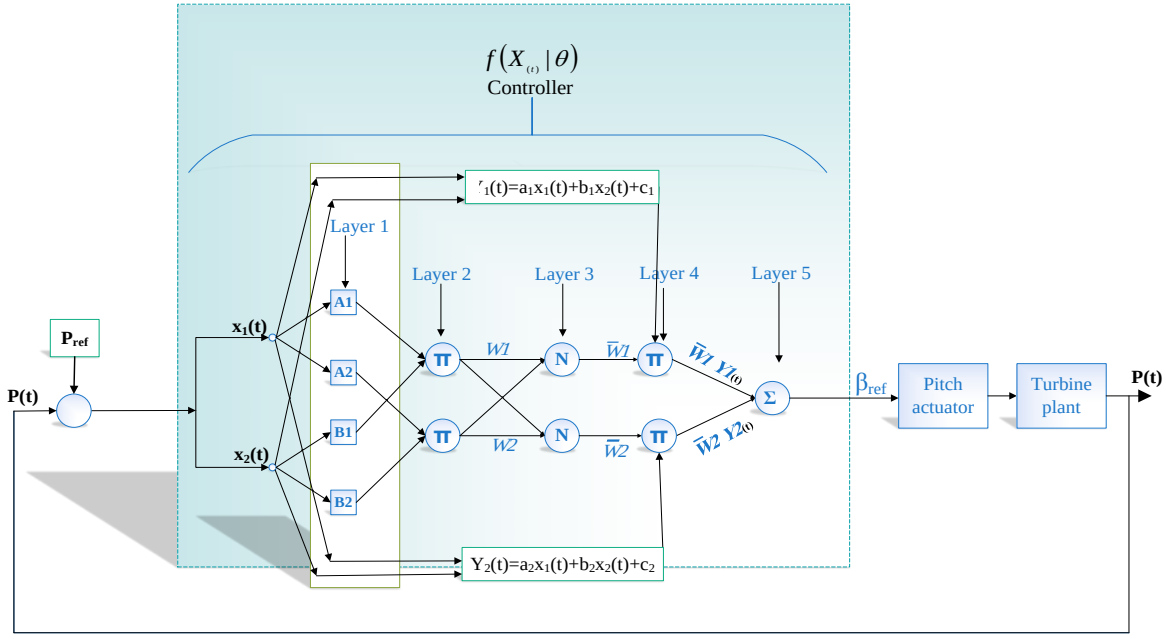

Figure 3. Structure of the ANFIS pitch controller.

4. THE PROPOSED CONTROLLERS

4.1. Neuro-fuzzy-PSO

For determining weight coefficients, the generator power, rotor speed, and the pitch angle are received from the PI controller. The elementary FIS is built through the FCM algorithm, and the cost function is optimized using the PSO method. In order to tackle the uncertainty, the neuro-fuzzy based clustering is repeated again. In this step, Δp and its integral are considered as the inputs of the ANFIS controller. The tunable inputs and output parameters of the ANFIS, which are optimized by the PSO algorithm, are presented in Table 1.

Table 1. Parameters of ANFIS.

Parameters / MF	σ		C		A	B	C
	IN1	IN2	IN2	IN3	Output		
MF1	0.03126	0.4257	-0.1443	0.2367	-1.97	-0.01401	-0.179
MF2	0.05946	0.3604	-0.1961	-0.8839	0.06527	-0.01237	-0.05713
MF3	0.04844	0.4376	0.9568	0.3038	15.58	-0.05776	0.4481
MF4	0.01322	0.5719	0.000495	-2.06	15.79	0.01269	0.5028
MF5	0.007274	0.3709	-0.03453	-0.523	41.02	0.0325	1.088
MF6	0.0445	0.3745	0.06928	-1.077	14.1	-0.00905	0.4965

4.2. RANFIS

For designing an orientated controller in line with the nonlinear nature of the system and converge more nonlinear modes of the system, RANFIS is suggested. To achieve a recurrent structure, after the completion of the training process, the controller commands feedback is applied as the

input. In this study, the delay of the pitch angle is applied as an input's controller together with the error of mechanical power and its delay. Table 2 shows input and output tunable parameters in RANFIS, where parameters are optimized through PSO.

Table 2. Parameters of RANFIS.

Parameters / MF	σ			C			A	B	C	D
	IN1	IN2	IN3	IN1	IN2	IN3	Output			
MF1	0.03943	-0.0071	0.5245	0.1138	0.1925	1.961	103.9	-59.76	0.4912	-5.141
MF2	0.07687	0.07471	0.4428	0.04911	0.04174	0.9684	16.2	-16.15	0.9962	0.0029
MF3	0.205	0.2059	0.4598	-0.1734	-0.1739	-0.033	0.1968	-0.1937	0.9892	0.00014

4.3. G.S RANFIS

In this part, the PI parameters are determined by determining the minimum error in the cost function. The proposed controller has two outputs to change online the proportion and integrator gains in the best cost function. Delay of the pitch angle is used as an input's controller, next to the error of mechanical power and its delay to cover more nonlinear modes. Table 3 and 4 shows the input and output of tunable parameters in G-S RANFIS optimized thorough PSO in the proposed wind turbine in the simulation. The block diagram of the RANFIS with the gain scheduling pitch angle controller is shown in Figure 4.

Table 3. Input parameters of G-S.RANFIS.

Parameters / MF	σ			C		
	IN1	IN2	IN3	IN1	IN2	IN3
MF1	0.1187	0.1671	0.7548	0.03239	-0.0383	-0.075
MF2	-0.0538	-0.0459	0.234	0.03017	-0.0031	0.8434
MF3	-0.0210	0.151	0.3051	-0.0228	-0.02581	0.1606

Table 4. Output parameters of G-S.RANFIS.

Parameters / MF	A		B		C		D	
	OUT1	OUT2	OUT1	OUT2	OUT1	OUT2	OUT1	OUT2
MF1	-0.572	-0.178	1.936	0.206	0.00907	-0.794	0.04485	0.03141
MF2	-0.935	-0.487	2.409	-0.556	0.1289	0.2509	-0.0198	0.04576
MF3	0.9889	-0.386	0.6147	-0.818	-0.0193	-0.337	-0.0346	-0.0020

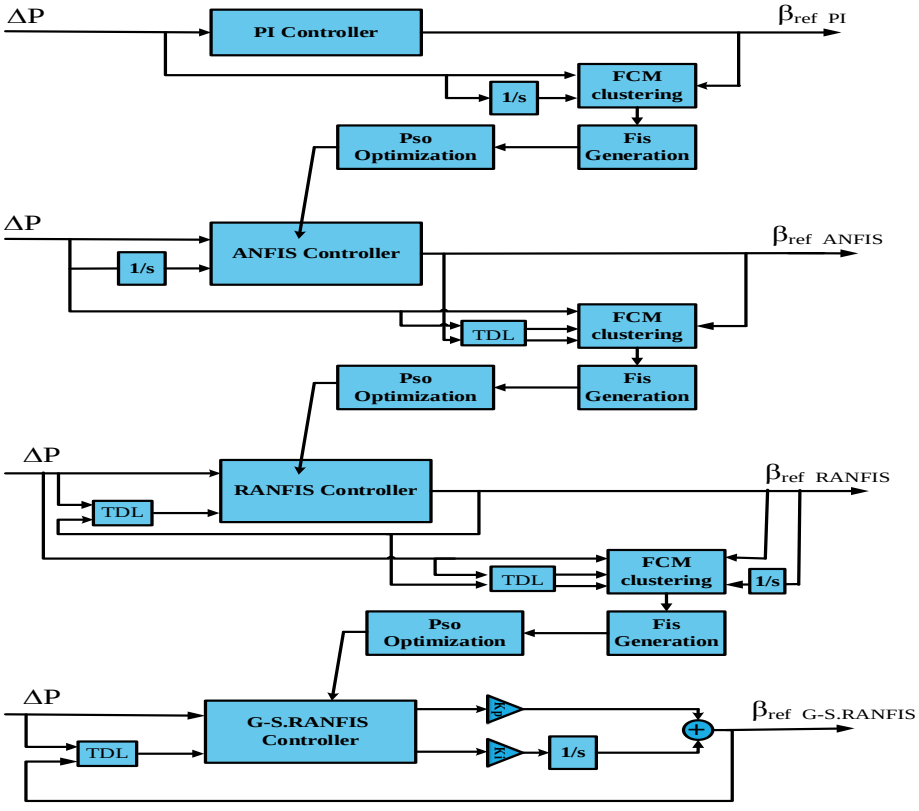

Figure 4. Block diagram of the proposed controllers: Using previous data's controller in each step.

5. SIMULATION RESULTS

In order to verify the efficiency of the proposed controllers, an induction generator in wind power system is considered for running the relevant simulations. The line length is 25 Km. The proportional and integral gains of the pitch angle controller are 5 and 25, respectively. The voltage of the infinitive bus is 25 KV, the grid voltage is 575 V, and the frequency is 60 Hz. The nominal power is 3 MW. The rated power and wind speed of the wind turbine are 3 MW and 11 m/s, respectively. The cut-out speed is 24 m/s, and the maximum and rated pitch angles are 45^{o} and 2^{o}/sec, respectively. As shown in Figure (5-a), a step-wise increasing wind pattern is inserted into the system for analyzing the pitch values calculated for the proposed wind turbine system.

As for the fluctuating wind speed, it is observed in Figure (5-b) that the output power also has many fluctuations due to the dependency of the generated power on the wind speed pattern. Thus, for evaluating the proposed controller, a reference response is required. Here, by comparing output power and pitch angle response to a linear wind pattern (Figure (5-a)), the best angle of blades is achieved and tabulated in Table 5.

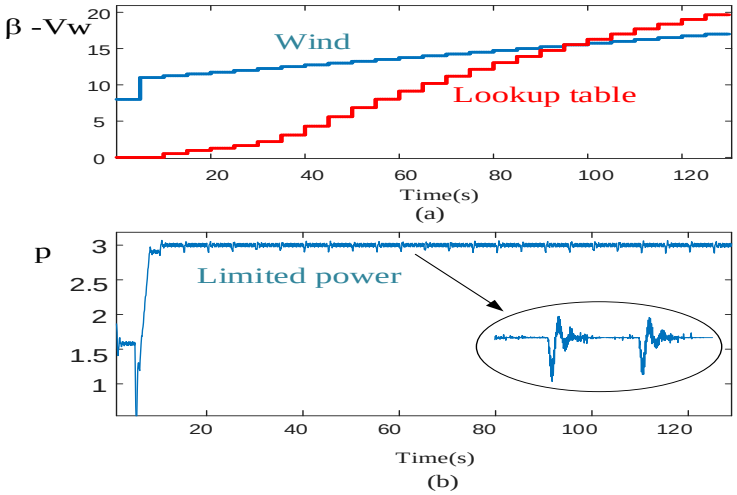

Figure 5. Lookup table response, (a) Pitch angle, (b) Output power.

Table 5. Lookup table parameters.

V_w	β	V_w	β	V_w	β	V_w	β	V_w	β	V_w	β
11	0	12	1.6266	13	5.599	14	10.196	15	13.917	16	17.011
11.25	0.5134	12.25	2.1709	13.25	6.846	14.25	11.197	15.25	14.745	16.25	17.705
11.5	0.9655	12.5	3.082	13.5	8.025	14.5	12.148	15.5	15.534	16.5	18.375
11.75	1.2685	12.75	4.309	13.75	9.135	14.75	13.055	15.75	16.286	16.75	19.02

The rated value of the wind speed shown in Figure 6 is 11 m/s. The wind pattern covers both the MPPT and pitch angle sectors to verify the performance of the controller.

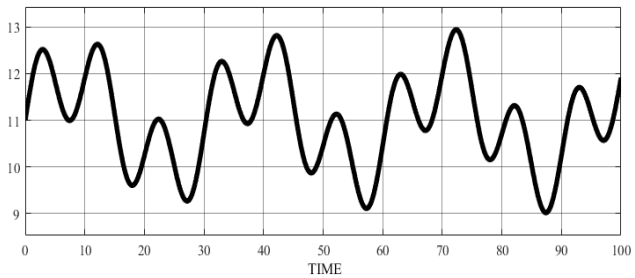

Figure 6. Wind speed pattern with a mean of 11m/s.

According to the increase of the pitch angle, as shown in Figure 7, the generator output power is kept at 3MW. Figure 8 shows the generator power, where it is limited under 3-MW by the proposed pitch controllers. As can be seen, the G-S RANFIS controller outperforms other controllers.

The rotor speed and the mechanical torque for different methods are shown in Figures 9 and 10, respectively. It is observed that the proposed scheme is capable of keeping the power coefficient near the optimal value; therefore, the desired rotor speed is determined better than common pith control methods.

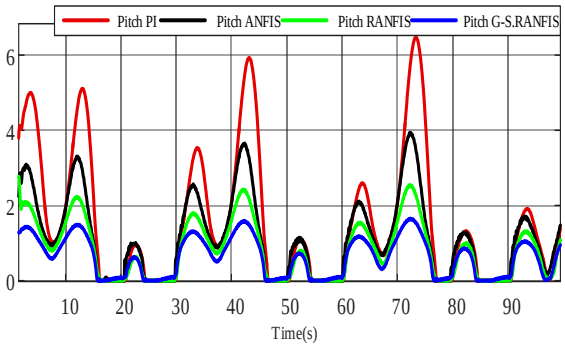

Figure 7. Pitch angle (deg).

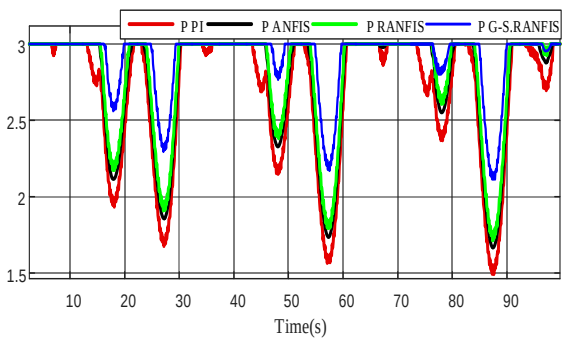

Figure 8. Generator power (MW).

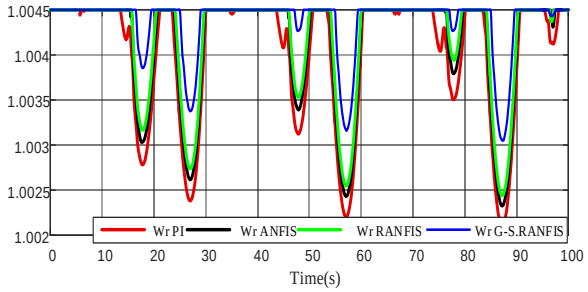

Figure 9. Rotor speed (pu).

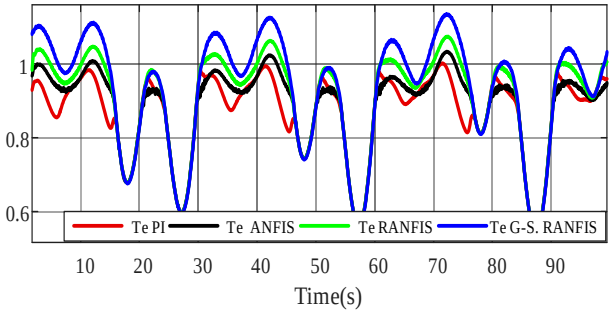

Figure 10. Mechanical torque (pu).

Figure 11 illustrates the power conversion coefficients of different controllers, where a maximum of Cp(max)=0.48 is calculated with a zero-pitch angle, which corresponds to λopt.

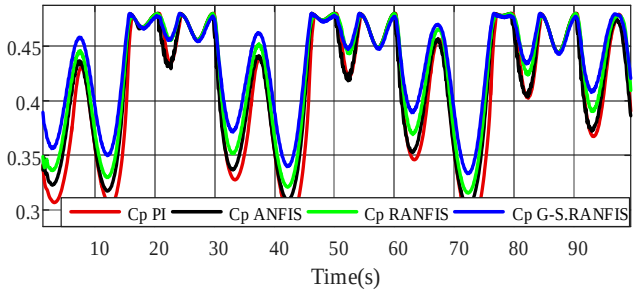

Figure 11. Power conversion coefficients.

Finally, the average generator power for the three methods in the full-load region is calculated and presented in Table 6, where the G-S RANFIS yields the highest output power. In this table, the improvement in the mean of P_{mec} and C_p is compared in percentage. It is shown that considering the pitch angle as a controller input and well clustering the data can greatly facilitate the achievement of the best pitch angle controll performance.

Table 6. Induction generator and grid parameters.

Mean	PI	ANFIS	RANFIS	G-S.RANFIS
Pmec (pu)	0.8450	0.8595	0.8836	0.9053
Cp	0.4102	0.4158	0.4262	0.4344

6. Validation of results

The objective controller is also evaluated by a more detailed model, the Fatigue, Aerodynamics, structures, and Turbulence (FAST7) model, which is capable of predicting both the extreme and fatigue loads of two and three bladed horizontal-axis wind turbines and is suitable for verifying and testing wind turbine control. The parameters of the FAST model are tabulated in Table 7, and Configuration of test pitch angle controller using FAST is shown in Fig. 12.

Table 7. FAST parameters.

Parameters	Value
Generator efficiency	100
Gearbox ratio	22.5
Rated generator slip percentage	1.5125 %
Synchronous (zero-torque) generator speed	1200 rpm
fixed rotor speed	54.333 rpm
Rated power	230 kw
P	1 kg/m^3
Radius	21.64 m

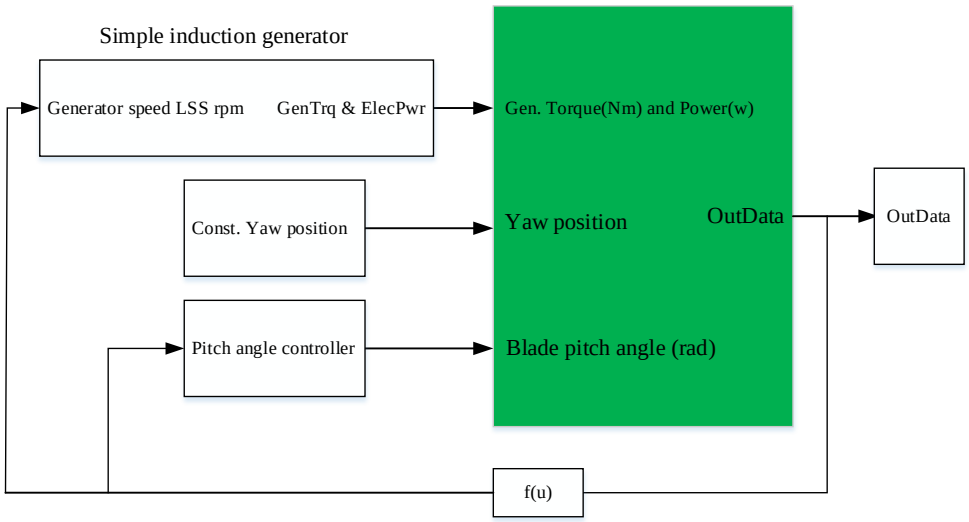

Figure 12. FAST nonlinear wind turbine.

Figures 13-16 show the configuration of the PI and G-S RANFIS in the FAST. By chosing a wind pattern upper and lower than the rated wind speed (Figure 13), both the MPPT and the pitch angle sectors are assessed. Figure 14 shows the rotor speed by time, which is fixed between its rated value when it is controlled by G-S RANFIS. The output G-S RANFIS control signal has less fluctuation than PI, as it is shown in Figure 15. The generator power and torque control are shown in Figures 16 a and b, respectively.

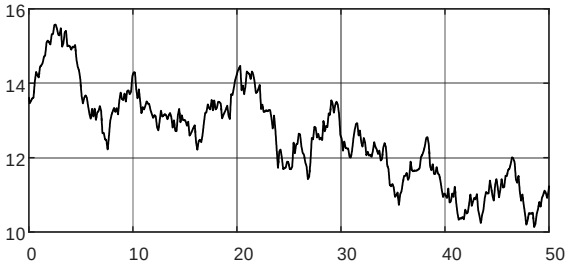

Figure 13. Wind speed.

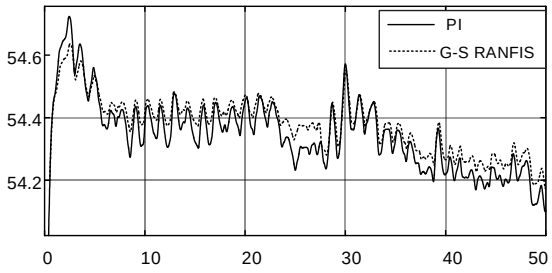

Figure 14. Rotor speed.

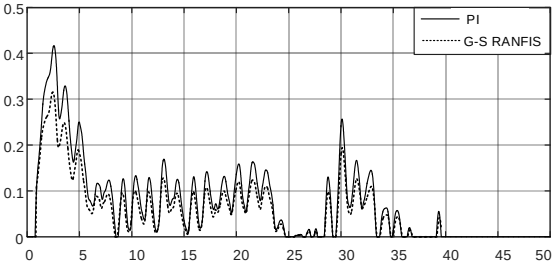

Figure 15. Output control signal.

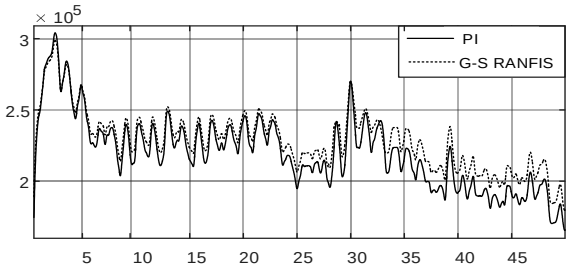

(a) Generator power

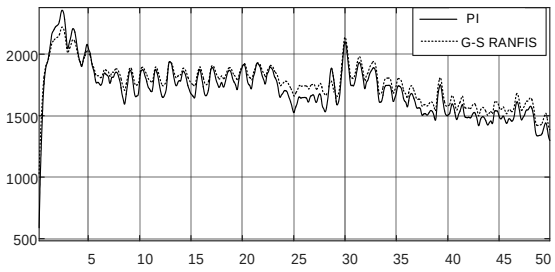

(b) Torque control

Figure 16. Generator power and torque control.

The power gained by the proposed controller is far greater than the PI due to the appropriate wind tracking at different times. Compared with the response of the two-mass model, the FAST simulation results include many authentic dynamics and high-frequency noise due to the high change rate of the random wind speed with high turbulence. The G-S RANFIS pitch controller has a better control performance in the whole wind speed region, especially at high turbulence intensity.

7. CONCLUSIONS

In this paper, a new G-S RANFIS was introduced to control the pitch angle, implemented on a 3-MW induction generator wind turbine, and validated by the FAST simulator. The results of the proposed control method were compared with those of the typical PI, ANFIS, and RANFIS controllers. From the simulation results, it can be seen that the G-S RANFIS controller is superior to other controllers, especially when there are abrupt variations in the wind speed. By comparing the average values of the controllers at a mean wind speed of 11 m/s, it can be observed that, using the G-S RANFIS controller, the output power of the generator is about 60 KW more than the PI controller. Moreover, the power conversion coefficient is about 6 % higher than the PI controller. In the FAST simulator, the mean power for the G-S RANFIS is 223 Kw and for the PI is 212 Kw. Therefore, the presented method is capable of providing superior power and dynamic responses.

8. ACKNOWLEDGEMENT

The authors would like to thank the respected journal executive, journal editor, and referees for making suggestions to improve the quality of the paper. This research has been conducted in the Smart Microgrid Research Center, Najafabad Branch, Islamic Azad University, Najafabad, Iran.

REFERENCES

1. Lyu, X., Zhao, J., Jia, Y., Xu, Z. and Wong, K.P., "Coordinated control strategies of PMSG-based wind turbine for smoothing power fluctuations", ***IEEE Transactions on Power Systems***, Vol. 34, No. 1, (2019), 391-401. (doi:10.1109/TPWRS.2).
2. Shair, J., Xie, X., Wang, L., Liu, W., He, J. and Liu, H., "Overview of emerging subsynchronous oscillations in practical wind power systems", ***Renewable and Sustainable Energy Reviews***, Vol. 99, (2019), 159-168. (doi:10.1016/j.rser .2018.09.047).
3. Jafari, A. and Shahgholian, G., "Analysis and simulation of a sliding mode controller for mechanical part of a doubly-fed induction generator based wind turbine", ***IET Generation, Transmission and Distribution***, Vol. 11, No. 10, (2017), 2677-2688. (doi:10.1049/iet-gtd.2016.1969).
4. Shonhiwa, C. and Makaka, G., "Concentrator augmented wind turbines: A review", ***Renewable and Sustainable Energy Reviews***, Vol. 59, (2016), 1415-1418. (doi:10.1016/j. rser.2016.01.067).
5. Shahgholian, G. and Ebrahimi-Salary, M., "Effect of load shedding strategy on interconnected power systems stability when a blackout occurs", ***International Journal of Computer and Electrical Engineering***, Vol. 4, No. 2, (2012), 212-216. (doi:10.7763/IJCEE. 2012.V4.481).
6. Shahgholian, G., "Review of power system stabilizer: Application, modeling, analysis and control strategy", ***International Journal on Technical and Physical Problems of Engineering***, Vol. 5, No. 3, (2013), 41-52.
7. Bertašienė, A. and Azzopardi, B., "Synergies of wind turbine control techniques", ***Renewable and Sustainable Energy Reviews***, Vol. 45, (2015), 336-342. (doi:10.1016/ j.rser.2015.01.063).
8. Datta, U., Shi, J. and Kalam, A., "Primary frequency control of a microgrid with integrated dynamic sectional droop and fuzzy based pitch angle control", ***International Journal of Electrical Power and Energy Systems***, Vol. 111, (2019), 248-259. (doi: 10.1016/j.ijepes. 2019.04.001).
9. Mozafarpoor-Khoshrodi, S.H. and Shahgholian, G., "Improvement of perturbing and observe method for maximum power point tracking in wind energy conversion system using the fuzzy controller", ***Energy Equipment and Systems***, Vol. 4, No. 2, (2016), 111-122. (doi: 10.22059/EES.2016 .23031).
10. Song, D., Yang, J., Su, M., Liu, A., Cai, Z., Liu, Y. and Joo, Y.H., "A novel wind speed estimator-integrated pitch control method for wind turbines with global-power regulation", ***Energy***, Vol. 138, (2017), 816-830. (doi:10.1016/j.energy. 2017.07.033).

11. Johnson, S.J., Larwood, S., McNerney, G. and Dam, C.P., "Balancing fatigue damage and turbine performance through innovative pitch control algorithm", ***Wind Energy***, Vol. 15, No. 5, (2012), 665-677. (doi:10.1002/we.495).
12. Yang, B., Jiang, L., Wang, L., Yao, W. and Wu, Q.H., "Nonlinear maximum power point tracking control and modal analysis of DFIG based wind turbine", ***International Journal of Electrical Power and Energy Systems***, Vol. 74, (2016), 429-436. (doi:10.1016/j.ijepes.2015. 07.036).
13. Yang, G. and Hao, Z., "Fuzzy self-adaptive PID control of the variable speed constant frequency variable-pitch wind turbine system", ***Proceeding of the IEEE/ICSSE***, (2014), 124-127. (doi:10.1109/ICSSE. 2014.6887918).
14. Shahgholian, G. and Izadpanahi, N., "Improving the performance of wind turbine equipped with DFIG using STATCOM based on input-output feedback linearization controller", ***Energy Equipment and Systems***, Vol. 4, No. 1, (2016), 65-79. (doi:10.22059/EES.2016.20128).
15. Faiz, J., Hakimi-Tehrani, A. and Shahgholian, G., "Current control techniques for wind turbines: A review", ***Journal of Electromotion***, Vol. 19, No. 3-4, (2012), 151-168.
16. Abu Hussein, A. and Hasan Ali, M., "Comparison among series compensators for transient stability enhancement of doubly fed induction generator based variable speed wind turbines", ***IET Renewable Power Generation***, Vol. 10, No. 1, (2016), 116-126. (doi:10.1049/ iet-rpg.2015.0055).
17. Corradini, M.L., Ippoliti, G. and Orlando, G., "Fully sensorless robust control of variable-speed wind turbines for efficiency maximization", ***Automatica***, Vol. 49, No. 10, (2013), 3023-3031. (doi:10.1016/ j.automatica.2013.07.028).
18. Murdoch, A., Barton, R.S., Winkelman, J.R. and Javid, S.H., "Control design and performance analysis of a 6 MW wind turbine-generator", ***IEEE Transactions on Power Apparatus and Systems***, Vol. 102, No. 5, (1983), 1340-1347. (10.1109/TPAS.1983.318083).
19. Tang, X., Yin, M., Shen, C., Xu, Y., Dong, Z.Y. and Zou, Y., " Active power control of wind turbine generators via coordinated rotor speed and pitch angle regulation", ***IEEE Transactions on Sustainable Energy***, Vol. 10, No. 2, (2019), 822-832. (doi:10. 1109/TSTE. 2018.2848923).
20. Avello, A.J., Al-Hadithi, B.M., Garcia, M.I.G. and Rubio, J.M.L., "Difference equation matrix model (DEMM) for the control of wind turbines", ***Wind Energy***, Vol. 17, No. 1, (2014), 57-74. (doi:10.1049/ iet-rpg.2015.0239).
21. Abulanwar, S., Hu, W., Chen, Z. and Iov, F., "Adaptive voltage control strategy for variable-speed wind turbine connected to a weak network", ***IET Renewable Power Generation***, Vol. 10, No. 2, (2016), 238-249. (doi:10.1049/iet -rpg.2015.0239).
22. Viudez-Moreiras, D., Martin, I. and Martin-Sanchez, J.M., "A new pitch angle adaptive control design", ***Proceeding of the IEEE/ICUAS***, Orlando, FL. (2014), 928-935. (doi:10.1109/ ICUAS.2014.6842342).
23. Soliman, M., Malik, O.P. and Westwick, D.T., "Multiple model predictive control for wind turbines with doubly fed induction generators", ***IEEE Transactions on Sustainable Energy***, Vol. 2, No. 3, (2011), 215-225. (doi:10.1109/TSTE.2011. 2153217).
24. Njiri, J.G. and Söffker, D., "State-of-the-art in wind turbine control: Trends and challenges", ***Renewable and Sustainable Energy Reviews***, Vol. 60, (2016), 377-393. (doi:10.1016/ j.rser.2016.01.110).
25. Boukhezzar, B. and Siguerdidjane, H., "Nonlinear control with wind estimation of a DFIG variable speed wind turbine for power capture optimization", ***Energy Conversion and Management***, Vol. 50, No. 4, (2009), 885-892. (doi:10.1016/j.enconman.2009.01.011).
26. Hang, J., Zhang, J. and Cheng, M., "Application of multi-class fuzzy support vector machine classifier for fault diagnosis of wind turbine", ***Fuzzy Sets and Systems***, Vol. 297, (2016), 128-140. (doi: 10.1016/j.fss.2015.07.005).
27. Suganthi, L., Iniyan, S. and Samuel, A.A., "Applications of fuzzy logic in renewable energy systems: A review", ***Renewable and Sustainable Energy Reviews***, Vol. 48, (2015), 585-607. (doi:10.1016/j.rser. 2015.04.037).
28. El-Hawary, M.E.,Fuzzy theory in electric power systems, Wiley-IEEE Press eBook Chapters, (1998), 7-11.
29. Musyafa', A., Harika, A., Negara, I.M.Y. and Robandi, I., "Pitch angle control of variable low rated speed wind turbine using fuzzy logic controller", ***International Journal of Engineering and Technology***, Vol. 10, No. 5, (2010), 22-25. (doi:10.1109/DRPT.2008.4523867).
30. Van, T.L., Nguyen, T.H. and Lee, D.C., "Advanced pitch angle control based on fuzzy logic for variable-speed wind turbine systems", ***IEEE Transactions on Energy Conversion***, Vol. 30, No. 2, (2015), 578-587. (doi:10.1109/TEC. 2014.2379293).
31. Lin, W., Hong, C., Ou, T. and Chiu, T., "Hybrid intelligent control of PMSG wind generation system using pitch angle control with RBFN", ***Energy Conversion and Management***, Vol. 52, No. 2, (2011), 1244-1251. (doi:10.1016/j.enconman. 2010.09.020).
32. Asghar, A.B. and Liu, X., "Estimation of wind turbine power coefficient by adaptive neuro-fuzzy methodology", ***Neurocomputing***, Vol. 238, (2017), 227-233. (doi:10.1016/j. neucom.2017.01.058).
33. Hosseini, E. and Shahgholian, G., "Output power levelling for DFIG wind turbine system using intelligent pitch angle control", ***Automatika***, Vol. 58, No. 4, (2017), 363-374. (doi:10.1080/00051144. 2018.1455017).
34. Lin, F.J., Hwang, J.C., Tan, K.H., Lu, Z.H. and Chang, Y.R., "Intelligent control of doubly-fed induction generator systems using PIDNNs", ***ASIAN Journal of Control***, Vol. 14, No. 3, (2012), 768-783. (doi:10.1002/asjc.426).
35. Shahgholian, G., "Modeling and simulation of a two-mass resonant system with speed controller", ***International Journal of Infoarmation and Electronics Engenieering***, Vol. 3, No. 4, (2013), 365-369. (doi: 10.7763/IJIEE.2013. V3.355).
36. Guo, W., Xiao, L. and Dai, S., "Fault current limiter-battery energy storage system for the doubly-fed induction generator: analysis and experimental verification", ***IET Generation, Transmission and Distribution***, Vol. 10, No. 3, (2016), 653-660. (doi:10.1049/iet-gtd.2014.1158).
37. Yang, L., Xu, Z., Ostergaard, J. and Dong, Z.Y., "Advanced control strategy of DFIG wind turbines for power system fault ride through", ***IEEE Transactions on Power Systems***, Vol. 27, No. 2, (2011), 713-722. (doi:10.1109/TPWRS. 2011.2174387).
38. Song, Y.D., Dhinakaran, B. and Bao, X.Y.,"Variable speed control of wind turbines using nonlinear and adaptive algorithms", ***Journal of Wind Engineering and Industrial Aerodynamics***, Vol. 85, No. 3, (2000), 293-308. (doi:10.1016/S0167-6105(99)00131-2).
39. Hu, L., Xue, F., Qin, Z., Shi, J., Qiao, W., Yang, W. and Yang, T., "Sliding mode extremum seeking control based on improved invasive weed optimization for MPPT in wind energy conversion system", ***Applied Energy***, Vol. 248, (2019), 567-575. (doi: 10.1016/ j.apenergy.2019.04.073).
40. Lin, W.M., Hong, C.M., Ou, T.C. and Chiu, T.M., "Hybrid intelligent control of PMSG wind generation system using pitch angle control with RBFN", ***Energy Conversion and Management***, Vol. 52, No. 2, (2011), 1244-1251. (doi:10.1016/j.enconman.2010.09.020).
41. Singh, M. and Chandra, A., "Application of adaptive network-based fuzzy inference system for sensorless control of PMSG-based wind turbine with nonlinear-load-compensation capabilities", ***IEEE Transactions on Power Electronics***, Vol. 26, No. 1, (2011), 165-175. (doi:10.1109/ TPEL.2010. 2054113).
42. Soliman, M., Malik, O.P. and Westwick, D.T., "Multiple model multiple-input multiple-output predictive control for variable speed variable pitch wind", ***IET Renewable Power Generation***, Vol. 5, No. 2, (2011), 124-136. (doi:10.1049/iet-rpg.2009.0137).
43. Muhando, E.B., Senjyu, T., Uehara, A., Funabashi, T. and Kim, C.-H., "LQG design for megawatt-class WECS with DFIG based on functional model's fidelity prerequisites", ***IEEE Transactions on Energy Conversion***, Vol. 24, No. 4, (2009), 893-904. (doi:10.1109/TEC.2009. 2025338).
44. Aghadavoodi, E. and Shahgholian, G., "A new practical feed-forward cascade analyze for close loop identification of combustion control loop system through RANFIS and NARX", ***Applied Thermal Engineering***, Vol. 133, (2018), 381-395. (doi: 10.1016/j.applthermaleng.2018. 01.075).
45. Jiang, F., Dong, L., Dai, Q. and Charles Nobes, D., "Using wavelet packet denoising and ANFIS networks based on COSFLA optimization for electrical resistivity imaging", ***Fuzzy Sets and Systems***, Vol. 337, (2018), 93-112. (doi: 10.1016/j.fss.2017.07.009).
46. Boutoubat, M., Mokrani, L. and Machmoum, M., "Control of a wind energy conversion system equipped by a DFIG for active power generation and power quality improvement", ***Renewable Energy***, Vol. 50, (2013), 378-386. (doi:10.1016/ j.renene.2012.06.058).
47. Shahgholian, G. and Movahedi, A., "Coordinated control of TCSC and SVC for system stability enhancement using ANFIS method",

International Review on Modelling and Simulations, Vol. 4, No. 5, (2011), 2367-2375.

48. Wei, M., Bai, B., Sung, A.H., Liu, Q., Wang, J. and Cather, M.E., "Predicting injection profiles using ANFIS", ***Information Sciences***, Vol. 177, No. 20, (2007), 4445-4461. (doi:10.1016/j.ins.2007.03.021).
49. Fattahi, H., "Adaptive neuro fuzzy inference system based on fuzzy c-means clustering algorithm, a technique for estimation of tbm penetration rate", ***International Journal of Optimization in Civil Engineering***, Vol. 6, No. 2, (2016), 159-171.
50. Sheikhan, M., Shahnazi, R. and Yousefi, A.N., "An optimal fuzzy PI controller to capture the maximum power for variable-speed wind turbines", ***Neural Computation and Application***, Vol. 23, No. 5, (2012), 1359-1368. (doi: 10.1016/j. energy.2016.03.095).